Co-Pyrolysis of Waste Printed Circuit Boards With Iron Compounds for Br-Fixing and Material Recovery

Weifang Chen (chenweifang@usst.edu.cn)
University of Shanghai for Science and Technology
Yongkai Shu
University of Shanghai for Science and Technology
Yonglun Li
University of Shanghai for Science and Technology
Yanjun Chen
University of Shanghai for Science and Technology
Jianbo Wei
University of Shanghai for Science and Technology

Research Article

Keywords: waste printed circuit board, co-pyrolysis, iron compuonds, Br-fixing, liquid yield

Posted Date: June 14th, 2021

DOI: https://doi.org/10.21203/rs.3.rs-544878/v1

Version of Record: A version of this preprint was published at Environmental Science and Pollution Research on July 27th, 2021. See the published version at https://doi.org/10.1007/s11356-021-15506-w.

Co-pyrolysis of waste printed circuit boards with iron compounds for Br-fixing and material recovery

Weifang Chen*, Yongkai Shu, Yonglun Li, Yanjun Chen, Jianbo Wei

School of Environment and Architecture, University of Shanghai for Science and Technology, 516 Jun Gong Road, Shanghai 200093, China

*Corresponding author email: chenweifang@usst.edu.cn

Abstract Waste printed circuit board was co-pyrolyzed with iron oxides and iron salts. Solid, liquid and gaseous products were collected and characterized. Co-pyrolysis with $FeCl_2$, $FeCl_3$ or $FeSO_4$ was able to increase the yield of liquid product which was rich in phenol and its homologues. Also, the addition of co-pyrolysis reagents reduced the release of brominated organics to liquid as Br was either fixed as $FeBr_3$ in solids or released as HBr. In particular, $FeCl_2$ showed the best ability to reduce the release of Br-containing organics to liquid compared with $FeCl_3$ and $FeSO_4$. Solid residuals were rich in iron oxides, glass fibers and charred organics with surface areas of 20.6-26.5 m^2/g. CO_2 together with a small amount of CH_4 and H_2 were detected in the gaseous products. Overall, co-pyrolysis could improve the quantity and quality of liquid oil which could be reused as chemical or energy sources. Pyrolysis of waste printed circuit board was promising as a method for recycling.

Keywords: waste printed circuit board, co-pyrolysis, iron compuonds, Br-fixing, liquid yield

1. Introduction

Generation of electronic waste worldwide has been growing consistently in recent years due to rapid technological advancements and short life span of electrical and electronic equipment (Zhu et al. 2020). As an import part of electrical and electronic equipment, printed circuit boards contained resources of high value including copper, tin, gold and silver etc. In general, it contained 20-30% metals, about 20% plastics while ceramics and glass fiber making up the rest (Nekouei et al. 2020).

Traditionally, after electronics reached their life span, the waste printed circuit

boards (WPCB) were separated and undergone a rough recovery of profitable metals (Cu, Au etc.) before they were disposed by landfill or incineration which could lead to serious contamination of air, soil and water (Mdlovu et al. 2018). In recent years, China has tightened its regulations on WPCB disposal after many reports of pollution by toxic metals and hazardous organic substances remained in WPCB. Effective recovery of metal resources (such as iron and copper) and non-metal fractions (such as resins) could reduce not only the environmental impact of WPCB but also the demand on natural ores (Hao et al. 2020).

One of the difficulties in WPCB recycling was its complex composition. It contained a wide range of organic and inorganics which varied according to device type, manufacturers etc. Bazargan (2014) reported that WPCB could contain up to 40 kinds of metals (e.g. Cu, Fe, Al, Sn, Ag, Au) and 10 kinds of non-metals. Some of the metal contents were even higher than mineral ores. Therefore, WPCB had great economic potential. Recovery of metals was usually more attractive due to it high added-value. With the advancement in research, the less valuable non-metallic fraction could also be recycled as a source of materials and energy (Ghosh et al. 2015; Shen et al 2018).

For recycle, WPCB was first disassembled manually or automatically to remove batteries and capacitors components. Then it was shredded, crush or ground/pulverized before physical, chemical and biological processes to further separate and enrich metals from resin, fiber glass and plastics (Shen et al. 2018). Physical separation methods could be shape-, density-, conductivity- or magnetism-based (Salbidegoitia et al. 2015). Other processes investigated extensively to recycle metals or non-metals included

gasification (Shen et al. 2018), supercritical fluid treatment (Golzary and Abdoli 2020), dissolution in organic solvents (Yousef et al. 2018), hydrometallurgical and pyrometallurgical techniques (Zhou et al. 2011; Qiu et al. 2020), pyrosis (Kim et al. 2018) and hydrothermal treatment (Yin et al. 2011).

As a waste disposal method for WPCB, pyrolysis was able to recycle both metals and organic matters. It was carried out under non-oxygen atmosphere and organics were decomposed into small molecular products. Metals was not oxidized under inert atmosphere and became easier to be liberated after pyrolysis while organics were converted to fuel or other valuable chemicals (Liu et al. 2021). Kim et al. (2015) reported that phenols and bisphenol A are the dominant compounds in the liquid phase products in pyrolysis of epoxy-PCB and paper-laminated phenolic printed board. Rajagopal et al. (2016) used physical activation on char obtained from pyrolysis and obtained activated carbon with a surface area as high as 700 m^2/g. Also, pyrolysis was carried out under relatively low temperature and normal pressure which means low energy consumption and cost (Shen et al. 2018).

However, WPCB contained many halogenated compounds as flame retardant. Among them, the most common is brominated compounds. The degradation of these compounds was found to produce toxic products such as dibenzo-p-dioxin, dibenzo-furan, 2-bromophenol, 2,6-dibromophenol and methyl bromide etc. (Ning et al. 2017). Co-pyrolysis with various additives were investigated to minimize the contents of brominated compounds in pyrolysis oil and gas (Ma et al. 2018). KOH, NaOH, K_2CO_3, $NaCO_3$, $CaCO_3$, La_2O_3, MgO, CuO, CaO, Al_2O_3, zeolite, iron oxides, carbon powder

have all been used as debrominated agents (Evangelopoulos et al. 2015). Shen (2020) reported that pretreatment of WPCB by alkali was better in Br fixing than alkali-salt. Br-fixing efficiency reached 53.6% by NaOH as Br released was adsorbed by NaOH to form NaBr and was retained in chars. Terakado et al. (2011) compared the debromination effects of metal oxides. The ability of oxides on HBr emission suppression varied. La_2O_3 and CaO were more effective with a suppression efficiency of about 90%. Br-fixing was achieved by bromination of oxides as LaOBr, $CuBr_2$, $CaBr_2$, $FeBr_2$ were found in the solid residues of pyrolysis. Many studies have shown that by choosing the right reagent, co-pyrolysis could not only reduce Br release into pyrolysis products but also induce higher yield of valuable oil or change the properties of solid residues (Kakria et al. 2020).

This research attempted to study the feasibility of WPCB recycling by co-pyrolysis with iron oxides and iron salts. Studies have shown that iron is a good catalyst for the graphitization of carbonaceous compounds. Wu et al. (2018) reported that Fe^{2+} or Fe^{3+} salts can be used as template and catalyst in their pyrolysis of phenol formaldehyde resin and ethylene glycol. Activation and pyrolysis worked together when $FeCl_2$ and $FeCl_3$ were added, leading to increase in yield and complete carbonization.

The WPCB herein was from Jiangsu Province, China. It was already disassembled, crushed and shredded with most of the electronic components and metals recovered. The residual WPCB, mainly non-metalic, was currently used as an additive in brick-making. However, the amount that could be consumed this way was limited by the demand for bricks. An additional outlet for the WPCB was urgently needed as landfill

was no longer an option while incineration was problematic in fear of dioxin emission.

This research focused on co-pyrolysis of WPCB with iron oxides and iron salts for the possibility of energy or materials recovery. Conditions of pyrolysis (temperature, mass ratio etc.) on the pyrolysis products were investigated in detail. In particular, the effects of different reagents (Fe_3O_4, $FeCl_2$, $FeCl_3$ and $FeSO_4$) on liquid yield, and characteristics of residual solids and liquid products were compared. Behavior of WPCB and reagents during pyrolysis were studied via the monitoring of crystalline phases, morphology, surface chemistry and elemental compositions. In addition, compositions of liquid products were investigated to study the Br-fixing behavior of different reagent.

2. Materials and methods

2.1 Materials

Waste printed circuit board (WPCB) used in this study was from a printed circuit board recycling company in Kunshan City, Jiangsu Province, China. Electronic components were disassembled first and a rough metal recovery was conducted by crushing and sorting. Therefore, the raw material in this study was mainly non-metallic with a residual metal content of 15.51%. Proximate analysis showed that WPCB contained 29.62% volatile carbon, 4.52% fixed carbon and 65.86% of ash.

Fig. 1 is a SEM image of the WPCB. It consists of particles and cylinder-shaped glass fiber. Particle size of the WPCB were mostly in the range of 10-200 μm.

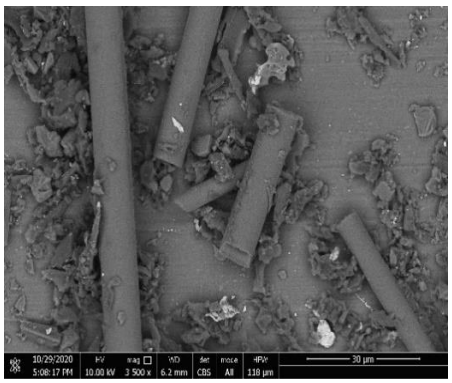

Fig. 1 SEM image of the original WPCB

Other materials used in the study, including $FeSO_4 \cdot 7H_2O$, $FeCl_2 \cdot 4H_2O$, $FeCl_3 \cdot 6H_2O$, and Fe_3O_4 were all purchased from Sinopharm Chemical Reagent Co.,Ltd. (Shanghai, China).

2.2 Pyrolysis

Pyrolysis of WPCB were carried out in a laboratory-scale tube furnace (OTF-1200X, Kejing, China) under nitrogen atmosphere. The reaction tube is 1000 mm in length and 54 mm in diameter. Fe_3O_4, $FeSO_4$, $FeCl_2$ and $FeCl_3$ were selected as reagents for co-pyrolysis. Co-pyrolysis of WPCB was carried out at temperatures ranging from 350-750°C. Fe_3O_4 in its powder form was mixed directly with WPCB. For co-pyrolysis with $FeCl_2$, $FeCl_3$ and $FeSO_4$, 10 g of WPCB were added to different volumes of solutions of 5 g/L then freezing dried to remove water. The $FeCl_2$, $FeCl_3$ and $FeSO_4$ to WPCB mass ratios were set at 0.25, 0.50 and 1.0. Before heating, the furnace was purged for air with N_2 at a rate of 10.0 mL/min for 30 min. Temperature was raised at a rate of 10°C/min. Time of pyrolysis was kept constant at 60 min. The outlet of tube furnace was connected to a condenser with cooling system to collect liquid oil. The remaining gas passed through dilute NaOH solution before exhaust was collected. All pyrolysis

157 samples were done in triplets. Results given were the averages.

158 Liquid yield (in percentage) was calculated as the mass of liquid collected divided
159 by mass of initial WPCB. Co-pyrolyzed sample was named as WPCB/reagent-
160 temperature, such as WPCB/$FeCl_2$-650.

161 **2.3 Characterization of pyrolysis products**

162 Thermogravimetric analysis of WPCB was conducted via a Thermal Gravimetric
163 Analyzer (TGA, STA-8000, PerkinElmer, USA). X-ray diffraction analysis was carried
164 out by X-ray Diffractometer (Rigaku UItima IV, Japan) with a Cu-Kα radiation at 40
165 kV and 30 mA as 2θ ranged from 10° to 80°. FTIR (NICOLET iS10, ThermoScientific,
166 Germany) analysis was employed to characterize functional groups of solids.
167 Morphologies of solid particles were analyzed by Scanning Electron Microscopes
168 (Nova Nano 450, FEI and ZEISS Gemini 300, Germany). Proximate analysis of WPCB
169 was carried out according to ASTM standard method E1131-08. Composition of
170 pyrolysis liquid was analyzed via a Gas Chromatography-Mass Spectrometry (GC-MS,
171 7890/5975C, Agilent, USA). GC-MS was operated with a HP-5MS capillary column
172 (30m×0.32 mm×0.25m). The initial temperature of the oven is 40℃ and kept for 5 min
173 before temperature was raised to 260℃ at 5℃/min and keep at 260℃ for 20 min. The
174 carrier gas was helium with a constant flow of 1.0 mL/min.

175 **3. Results and discussion**

176 **3.1 Screening of co-pyrolysis reagent by liquid yield**

177 In this research, WPCB and WPCB mixed with iron compounds were pyrolyzed at
178 high temperature to investigate the effects of these additives. The compounds selected

were Fe_3O_4, $FeCl_2$, $FeCl_3$ and $FeSO_4$.

Fig.2 is the change in liquid yield of pyrolysis with the change of temperature and iron compound/WPCB ratio.

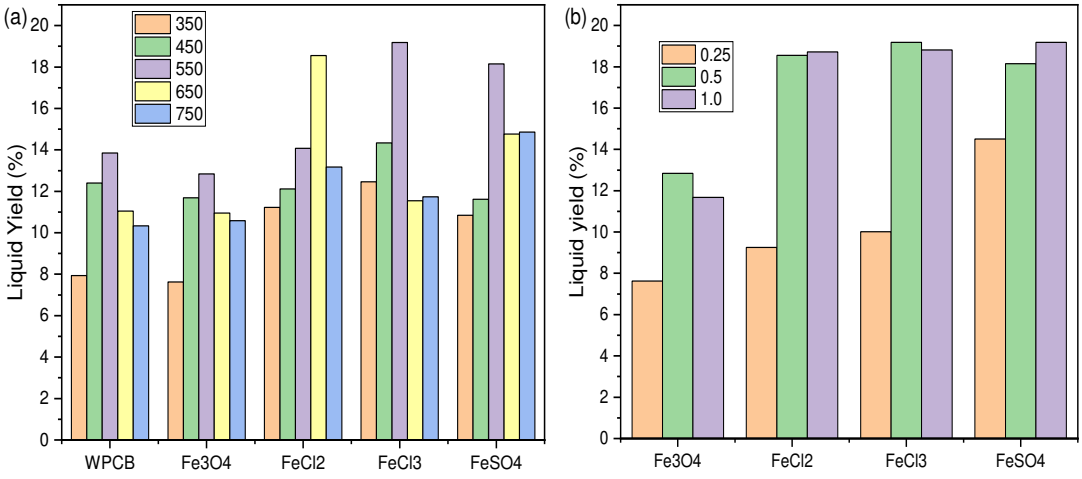

Fig.2 Liquid yield of WPCB with different iron compounds with the change of (a) temperature and (b) mass ratio

Studies have shown that liquid products from WPCB pyrolysis could be a valuable source of chemicals or energy as it contained products such as phenols and bisphenol A etc. (Quan et al. 2010; Gao et al. 2020). Fig.2(a) shows how liquid yield varied with temperature when different iron compounds were used. Iron compound/WPCB ratio was kept constant at 0.5. Liquid yield peaked at 550℃ for WPCB. The addition of Fe_3O_4 actually led to a slight drop in yield per unit of WPCB. In contrast, the addition of $FeCl_2$, $FeCl_3$ and FeSO4 was beneficial probably due to these iron salts' ability to catalyze graphitization of carbonaceous materials. The highest yield increased from 13% to around 18-20%. The optimal pyrolysis temperature was 550-650℃.

Iron compound/WPCB ratio also affected liquid generation (Fig. 2(b)). The pyrolysis temperature was set at 650℃ for $FeCl_2$ and 550℃ for the rest. There is a

general trend of increase in yield with the increase of mass ratio from 0.25 to 0.5. Higher ratio means more iron mass per unit of WPCB. The effects of mass levelled off after the ratio reached beyond 0.5 for $FeCl_2$, $FeCl_3$ and $FeSO_4$. This is in accordance with results from Gao et al. (2019). They also found there is an optimal mass ratio between iron oxide and WPCB for liquid yield from pyrolysis.

Next, pyrolysis behavior of WPCB with $FeCl_2$, $FeCl_3$ and $FeSO_4$ was investigated in detail.

3.2 Pyrolysis with $FeCl_2$

Fig.3 is the mass loss of WPCB, $FeCl_2$ and WPCB/$FeCl_2$ during pyrolysis at different temperature and XRD, FTIR and SEM images of the residual solids. The $FeCl_2$/WPCB ratio was set at 0.5. Fig.3(a) is the mass loss during pyrolysis. 20.8% of mass was lost when WPCB was pyrolyzed at 350℃ for 1 h. As pyrolysis temperature was raised from 450℃ to 750℃, mass loss increased only slightly from 22.6% to 24.7%. For comparison, mass loss of $FeCl_2$ in N_2 was also recorded in Fig.3. As temperature was raised, $FeCl_2$ was first converted to FeOOH which can further decomposed into iron oxides such as Fe_2O_3 with reactions (1) and (2) (Kang et al. 2010).

$$120-200℃: FeCl_2 \cdot 2H_2O \rightarrow FeOCl \cdot H_2O + HCl \rightarrow FeOOH + 3HCl \quad (1)$$

$$200-490℃: 2FeOOH \rightarrow Fe_2O_3 + H_2O \quad (2)$$

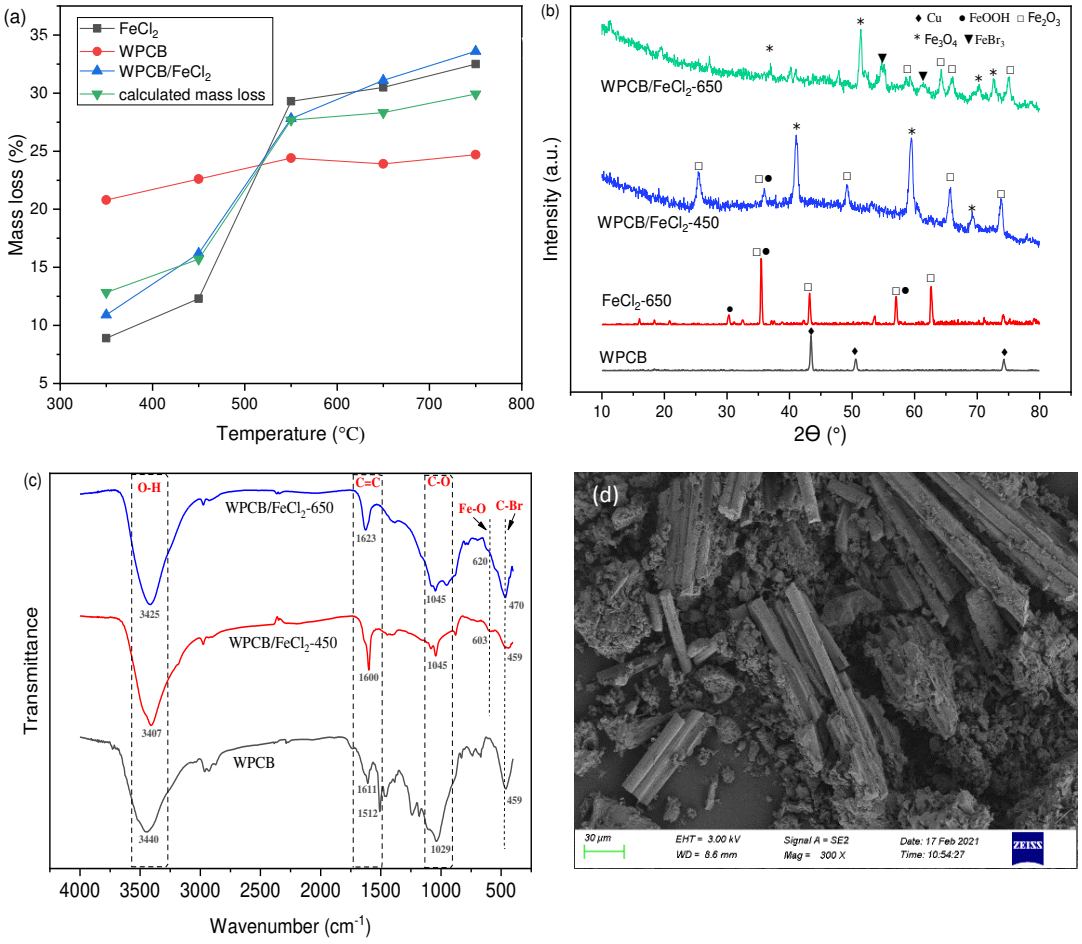

Fig. 3 Characterization of WPCB, $FeCl_2$ and WPCB/$FeCl_2$: (a) mass loss; (b) XRD; (c) FTIR; (d) SEM image of WPCB/$FeCl_2$-650

So mass loss was caused by $FeCl_2$ being converted to iron oxides. There is a sharp mass loss of $FeCl_2$ between 350-550°C. Calculated mass losses in Fig. 3 were obtained assuming mass change of WPCB and $FeCl_2$ in WPCB/$FeCl_2$ was independent of each other. Mass losses labelled as WPCB/$FeCl_2$ were the real values of WPCB/$FeCl_2$ mixture. Total mass loss ranged from 10.9-33.6% as compared to the calculated loss of 7.4-29.9%. Real mass losses were slightly higher than calculated ones. The higher mass loss could be due to interactions between WPCB and $FeCl_2$.

In their research using $FeCl_2$ as activating agents to recycle tomato stem waste, Fu et al. (2017) reported that Fe_2O_3 from $FeCl_2$ decomposition could be reduced by

charred organics to produce Fe_3O_4 or even Fe^0 (reactions (3) and (4))

$$> 490℃: 3Fe_2O_3 + C \rightarrow 2Fe_3O_4 + CO \quad (3)$$

$$700 - 800℃: Fe_3O_4 + C \rightarrow 3Fe^0 + 2CO_2 \quad (4)$$

It's possible the higher mass loss from WPCB/$FeCl_2$ was the result of reduction of Fe_2O_3 by carbon to Fe_3O_4 or Fe^0 in WPCB.

XRD, FTIR patterns and SEM images of WPCB/$FeCl_2$ residual solids were shown in Fig.3(b)-(d). XRD pattern (Fig.3(b)) showed Cu crystals in the raw WPCB. Fe_2O_3 was the main crystals found in thermal treatment of $FeCl_2$ at 650℃. FeOOH was also detected at 2θ of 28.9º. The results here were in accordance with those indicated in reactions (1) and (2). Fe_3O_4 was observed for WPCB/$FeCl_2$ mixture treated at 450℃ and 650℃ together with Fe_2O_3. This proved that Fe_2O_3 from $FeCl_2$ decomposition was reduced to form Fe_3O_4 when WPCB was present. Also, peaks at 2θ of 53º and 57º were believed to be those of $FeBr_3$. This means that Br from WPCB was fixed by $FeCl_2$ decomposition products. However, the absence of $FeBr_3$ in XRD patterns of 450℃ did not indicate no Br-fixing occurred. It only means the resultant $FeBr_3$ may not be crystalline.

Fig. 3(c) were the FTIR patterns. Peaks around 3440-3407 cm^{-1} were assigned to the vibration of O-H stretching (Ng et al. 2009). Bands at about 1400 -1600 cm^{-1} were the C=C vibration in the benzene ring skeleton while those at 1040^{-1} were attributed to the C-O stretching (Zhang et al. 2015). In addition, C-Br peaks were found in all samples at 459-471 cm^{-1} as brominated epoxy was commonly employed in WPCB as fire retardant while Fe-O peaks at 603-620 cm^{-1} were found only in WPCB/$FeCl_2$

pyrolyzed samples. Fig.3(d) is the SEM image of WPCB/$FeCl_2$ pyrolyzed at 650°C (WPCB/$FeCl_2$-650). WPCB consist mainly of cylindrical glass fibers and small particles. After pyrolysis with $FeCl_2$, glass fibers disintegrated due to the corrosive effects of HCl from $FeCl_2$ decomposition

3.3 Pyrolysis with $FeCl_3$

Fig. 4 is the mass loss, XRD, FTIR patterns and SEM image of WPCB pyrolyzed with $FeCl_3$.

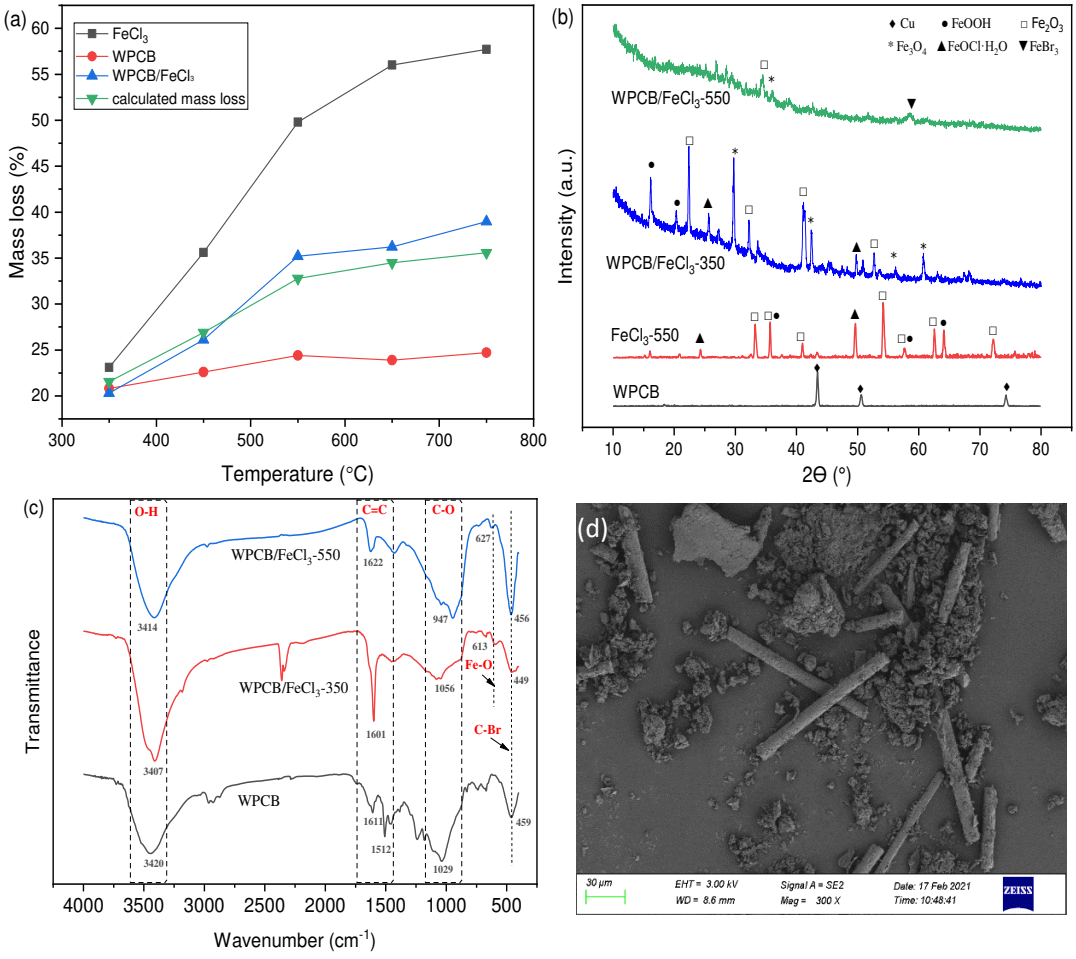

Fig. 4 Characterization of WPCB, $FeCl_3$ and WPCB/$FeCl_3$: (a) mass loss; (b) XRD; (c) FTIR; (d) SEM image of WPCB/$FeCl_3$-550

$FeCl_3$ was converted to FeOOH under high temperature (reactions (5)) which could then undergo further reactions such as reactions (1) and (2) above to form other iron

oxides (Xu et al. 2019).

$$200-330°C: FeCl_3 + 2H_2O \rightarrow FeOCl \cdot H_2O + 2HCl \rightarrow FeOOH + 3HCl \quad (5)$$

According to mass loss results in Fig. 4(a), $FeCl_3$ suffered continuous mass loss as temperature rose from 350℃ to 650℃ then plateaued. 55% of the original $FeCl_3$ was lost during thermal treatment. Mass losses of WPCB/$FeCl_3$ mixture varied from 20% to about 39% which was also slightly higher than the calculated mass losses. This could also be due to the interaction between iron oxides and carbon produced from WPCB pyrolysis as shown in reactions (3) and (4).

The reduction of Fe_2O_3 to Fe_3O_4 was proven by XRD patterns in Fig.4(b). Fe_3O_4 were detected in WPCB/$FeCl_3$ pyrolyzed at 350℃ and 550℃. As comparison, the dominant crystalline phases detected in $FeCl_3$ treated under N_2 at 550℃ were FeOOH and Fe_2O_3. Peaks at 2θ of 24.8º and 48.9º were ascribed to $FeOCl \cdot H_2O$. These were found in pyrolysis samples of $FeCl_3$ and WPCB/$FeCl_3$ treated at 350℃ but not samples treated at 550℃. This means that $FeOCl \cdot H_2O$ was an intermediate during decomposition which was converted at high temperature. In addition, $FeBr_3$ crystals were found in the solid residuals treated at temperature 550℃ probably due to reaction between Br from WPCB and iron oxides.

Fig. 4(c) were the FTIR patterns of original WPCB and two pyrolyzed WPCB/$FeCl_3$ samples. Peaks of O-H, C=C, C-O and C-Br structures were detected in all samples together with Fe-O structures. SEM image of WPCB/$FeCl_3$ treated at 550℃ showed glass fibers in cylindrical shapes but cavities were observed on the surface of glass giber indicating also that the addition of $FeCl_3$ led to the corrosion of glass fiber.

3.4 Pyrolysis with $FeSO_4$

Fig. 5 is the mass loss, XRD, FTIR and SEM analysis results WPCB pyrolyzed with $FeSO_4$.

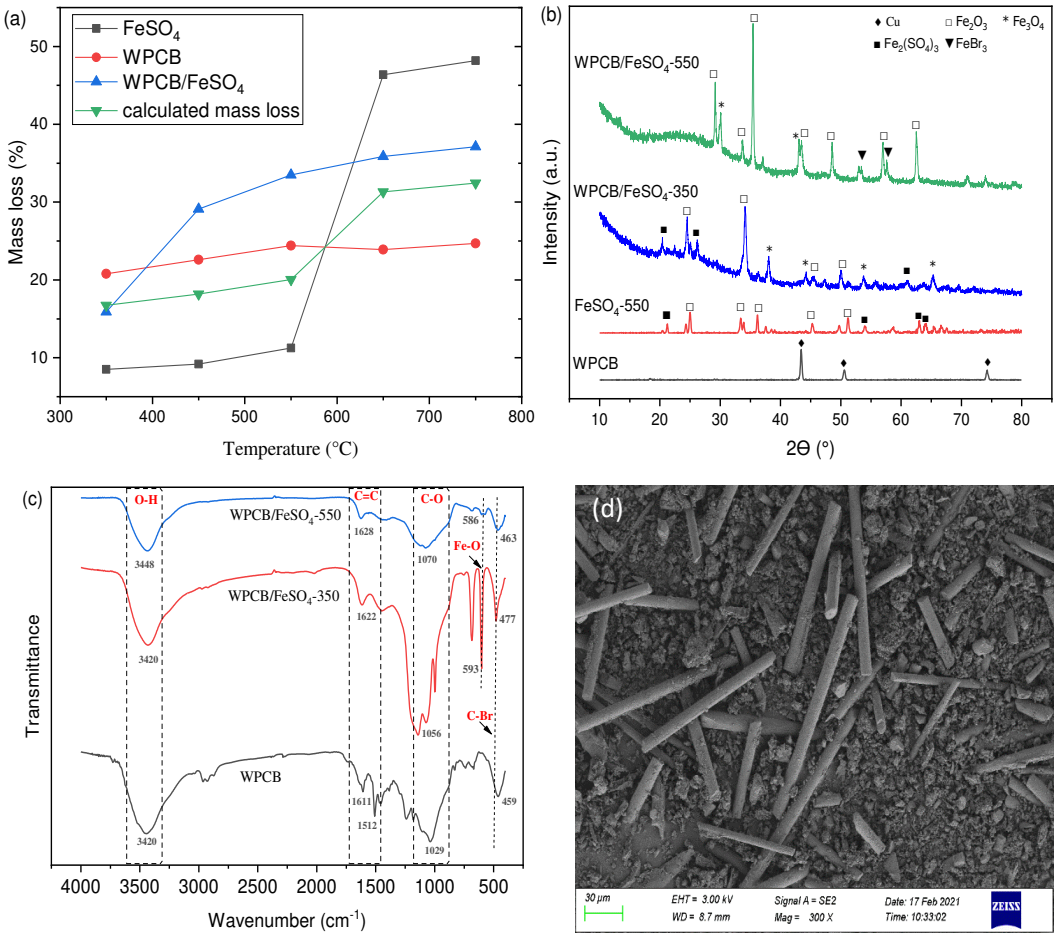

Fig. 5 Characterization of WPCB, $FeSO_4$ and WPCB/$FeSO_4$: (a) mass loss; (b) XRD; (c) FTIR; (d) SEM image of WPCB/$FeSO_4$-550

In their study on thermal decomposition of $FeSO_4 \cdot 6H_2O$, Masset et al. (2006) revealed that $FeSO_4 \cdot 6H_2O$ dehydrated step-wise from $FeSO_4 \cdot 6H_2O$ to $FeSO_4 \cdot 4H_2O$ to $FeSO_4 \cdot H_2O$ at temperature from 70-310°C. Decomposition of $FeSO_4$ to hematite (Fe_2O_3) occurred at high temperature (reactions (6) and (7)). $FeSO_4$ completely converted to $Fe_2(SO_4)_3$ and Fe_2O_3 at 550°C and $Fe_2(SO_4)_3$ was found to be the only intermediate compound during the decomposition. The mass loss by $FeSO_4$ under N_2

297 shown in Fig. 5(a) in this research correlated well with Masset et al.'s findings. Sharp
298 mass loss of $FeSO_4$ was recorded only when pyrolysis temperature was greater than
299 550℃.

300 $$525-650℃: 6FeSO_4 \rightarrow Fe_2(SO_4)_3 + 2Fe_2O_3 + 2SO_2 \quad (6)$$

301 $$527-710℃: 2FeSO_4 \rightarrow Fe_2O_3 + 2SO_2 + O_2 \quad (7)$$

302 X-ray diffraction was conducted to identify the crystalline phases formed during
303 pyrolysis. XRD pattern of $FeSO_4$ treated at 550℃ for 1 h in Fig. 5(b) showed the
304 presence of both $Fe_2(SO_4)_3$ and Fe_2O_3. These two phases were also detected with
305 WPCB/$FeSO_4$ treated at 350℃. In contrast, $Fe_2(SO_4)_3$ was not found in WPCB/$FeSO_4$
306 treated at 550℃ indicating a complete conversion to Fe_2O_3 at high temperature. $FeBr_3$
307 was present at WPCB co-pyrolyzed with $FeSO_4$ at 550℃ but not at sample of 350℃.

308 FTIR pattern were quite similar to those co-pyrolyzed with $FeCl_2$ and $FeCl_3$. Peaks
309 at 3420-3450 cm^{-1}, 1510 cm^{-1}, 1040-1070 cm^{-1}, 460-480 cm^{-1} were due to the vibration
310 of O-H, C=C, C-O and C-Br structures respectively. Fe-O vibrations were detected
311 around 590 cm^{-1}. SEM image of WPCB/$FeSO_4$ treated at 550℃ showed glass fibers
312 remaining cylindrical with very little disintegration. The corrosive effects of $FeSO_4$
313 was much less than those of $FeCl_2$ and $FeCl_3$.

314 Overall, co-pyrolysis of WPCB with $FeCl_2$, $FeCl_3$ and $FeSO_4$ generated solids with
315 different morphology and composition. Table 1 further lists the elemental composition,
316 pore volume and surface areas of these solids. About half of the carbon in raw WPCB
317 was lost during pyrolysis. The addition of $FeSO_4$ had resulted in obvious increase in S
318 content. Solid manifested certain porosity with surface areas about 20.6-26.5 m^2/g.

319 **Table 1** elemental analysis, total pore volumes and surface areas of pyrolyzed

320 solids

Sample	Elemental Analysis (%)				Total pore volume (cm^3/g)	BET Surface area (m^2/g)
	C	H	N	S		
WPCB	24.13	1.95	0.32	0.31	-	-
WPCB/$FeCl_2$-650	12.80	2.26	0.28	0.37	0.12	23.4
WPCB/$FeCl_3$-550	14.34	1.60	0.35	0.36	0.089	20.6
WPCB/$FeSO_4$-550	11.60	0.47	0.20	5.63	0.12	26.5

321

322 Pyrolysis changed physical and chemical properties of WPCB. Based on liquid yield,
323 it is optimal to conduct pyrolysis at mass ratio of 0.5 and temperatures of 550-650℃.
324 Part of Br was fixed as $FeBr_3$ crystals at these temperatures. The resultant solids consist
325 of chars, iron oxides and metals from raw WPCB and added reagents. Research on
326 recovering of residual metals (e.g. Cu), toxicity leaching and potential reuse of the
327 pyrolysis solids are currently underway. It could be a potential source of building
328 materials. Gao et al. (2019) used pyrolysis products as carbon and iron source to
329 synthesize magnetic carbon fibers.

330 **3.5 Characterization of liquid and gas products**

331 In addition to the characterization of solids, the composition of liquid products was
332 determined by GC-MS as shown in Fig.6. Liquids were collected from pyrolysis at
333 mass ratio of 0.5 and temperature of 650℃ for WPCB/$FeCl_2$ and 550℃ for WPCB,
334 WPCB/$FeCl_3$ and WPCB/$FeSO_4$. Phenol and its derivatives were identified as the main
335 products. Monitoring of liquid composition showed varied presence of brominated
336 organics with the addition of co-pyrolysis reagent. Pyrolysis of WPCB generated a
337 wealth of brominated organics including 2,4-dibromophenol and 2,4,6-tribromophenol,

2-bromo-4-methylphenol. In contrast, liquid products of $FeCl_2$ were dominated by phenol and no brominated organics compounds were detected. Chloride and bromide were released as HCl and HBr into the liquid phase as shown in Fig. 6(b). Brominated organics were also found when $FeCl_3$ and $FeSO_4$ were used. Particularly, co-pyrolysis with $FeCl_3$ actually led to the generation of chlorinated compound, i.e. 4-chloro-2-(1-methylethyl)phenol in Fig.6(c).

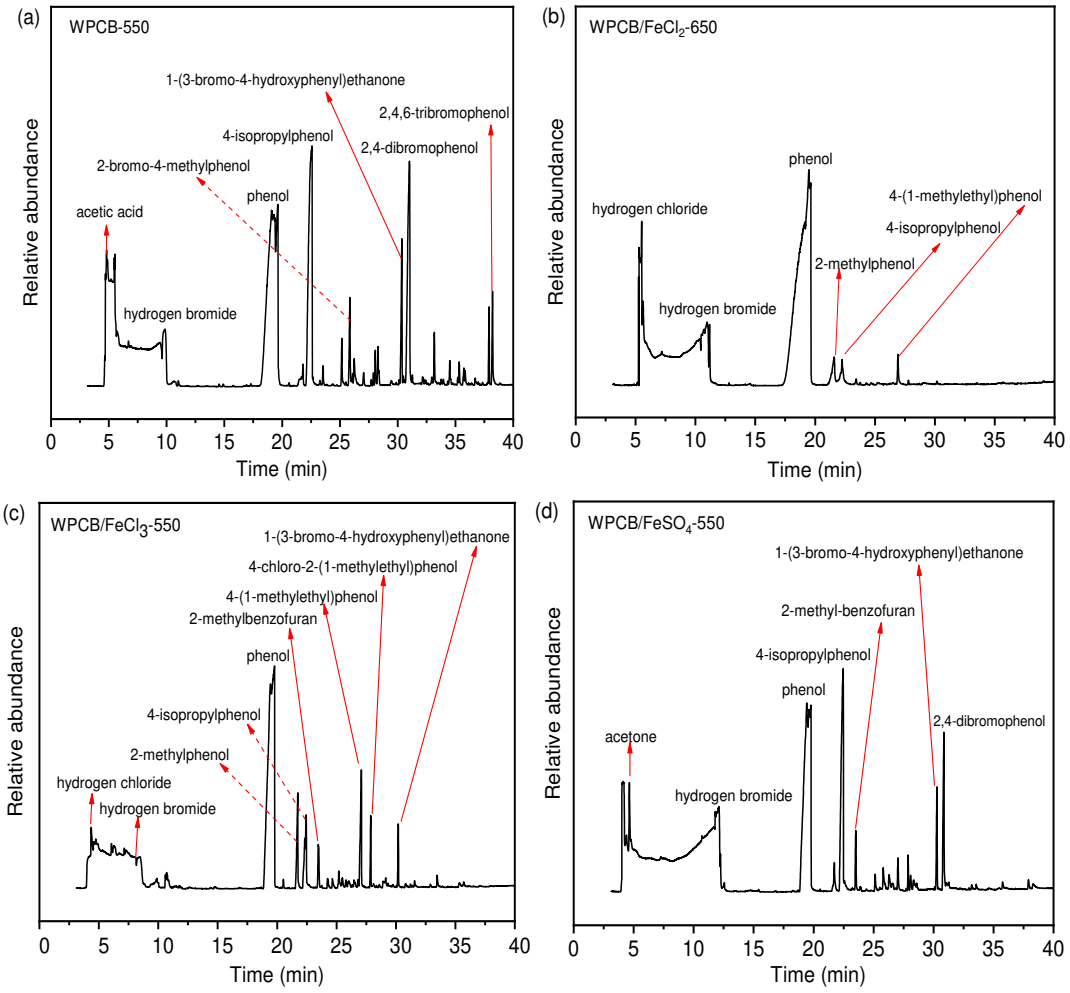

Fig.6 GC-MS results for pyrolysis liquid from (a) WPCB-550; (b) WPCB/$FeCl_2$-650; (c) WPCB/$FeCl_3$-550; (d) WPCB/$FeSO_4$-550

Compared with $FeCl_3$ and $FeSO_4$, conversion of $FeCl_2$ to FeOOH and HCl started at lower temperature (120-200°C) according to reaction (1). It is possible that the lack

of chlorinated products was due to the fact that Cl in $FeCl_2$ was quickly released at low temperature as HCl which prevented the formation of chlorinated products. At the same time, iron oxides thus generated acted as Br-fixing agent when Br-containing fire retardant started to degrade. Also, the addition of $FeCl_2$ suppressed the bromination of organics as Br released from fire retardant was either released as HBr or fixed as $FeBr_3$. The mechanism of Br-fixing will be further clarified by studying the mass balance of Br in future research. Based on the quantity and quality of liquid products, $FeCl_2$ could be recommended as a co-pyrolysis reagent.

In addition, pyrolysis exhaust was collected and analyzed. CO_2, CH_4 and H_2 were the main compounds detected. It appeared that no toxic gas was generated during pyrolysis.

4. Conclusions

WPCB was co-pyrolyzed with Fe_3O_4, $FeCl_2$, $FeCl_3$ and $FeSO_4$. Liquid yield was used as the screening factor which showed that the addition of $FeCl_2$, $FeCl_3$ and $FeSO_4$ was conducive to liquid production. The optimal mass ratio and temperatures were 0.5 and 550-650℃ for liquid yields which ranged from 18-20%. About half of the C in raw WPCB remained in solid phase and was present as chars. Iron compounds were decomposed to iron oxides at high temperature. Characterization of liquid by GC-MS revealed that phenol and its homologues are the main products which could be a valuable chemical source. $FeCl_2$, $FeCl_3$ and $FeSO_4$ showed different Br-fixing capacity. No brominated or chlorinated organics were found in liquid products from co-pyrolysis with $FeCl_2$. The addition of $FeCl_2$ suppressed the generation of brominated organics.

Br was either fixed as $FeBr_3$ in solids or released as HBr to liquid. In summary, the roles of co-pyrolysis reagent such as $FeCl_2$ were two-fold. First, it could improve the decomposition of macro-molecule in WPCB and increase liquid yield. Secondly, it reduced the bromination of organics and prevent excessive release of brominated organics.

Declarations

- Ethics approval and consent to participate

  Not applicable

- Consent for publication

  Not applicable

- Availability of data and materials

All data generated or analyzed during this study are included in this published article

- Author contributions

All authors contributed to the study conception and design. Material preparation, data collection and analysis were performed by Weifang Chen, Yongkai Shu, Yonglun Li, Yanjun Chen and Jianbo Wei. The first draft of the manuscript was written by Weifang Chen and Yongkai Shu. All authors commented on previous versions of the manuscript. All authors read and approved the final manuscript.

- Competing interests

The authors declare that they have no competing interests

- Acknowledgement

This work was supported by Shanghai Natural Science Foundation (14ZR1428900)

394 and National Natural Science Foundation of China (21707090).

395

396 **References**

397 Bazargan A, Bwegendaho D, Barford J, McKay G (2014) Printed circuit board waste
398 as a source for high purity porous silica. Sep Purif Technol 136: 88-93.
399 https://doi.org/10.1016/j.seppur.2014.08.026

400 Evangelopoulos P, Kantarelis E, Yang W (2015) Investigation of the thermal
401 decomposition of printed circuit boards (PCBs) via thermogravimetric analysis (TGA)
402 and analytical pyrolysis (Py-GC/MS). J Anal Appl Pyrol 115: 337-343.
403 https://doi.org/10.1016/j.jaap.2015.08.012

404 Fu K, Yue Q, Gao B, Wang Y, Li Q (2017) Activated carbon from tomato stem by
405 chemical activation with $FeCl_2$. Colloids Surf A 529: 842-849.
406 https://doi.org/10.1016/j.colsurfa.2017.06.064

407 Gao R, Zhan L, Guo J, Xu Z (2020) Research of the thermal decomposition
408 mechanism and pyrolysis pathways from macromonomer to small molecule of waste
409 printed circuit board. J Hazard Mater 383: 121234.
410 https://doi.org/10.1016/j.jhazmat.2019.121234

411 Gao R, Liu B, Xu Z (2019) Fabrication of magnetic zeolite coated with carbon fiber
412 using pyrolysis products from waste printed circuit boards. J Clean Prod 231: 1149-
413 1157. https://doi.org/10.1016/j.jclepro.2019.05.220

414 Ghosh B, Ghosh MK, Parhi P, Mukherjee PS, Mishra BK (2015) Waste printed circuit
415 boards recycling: an extensive assessment of current status. J Clean Prod 94: 5-19.

https://doi.org/10.1016/j.jclepro.2015.02.024

Golzary A, Abdoli MA, Recycling of copper from waste printed circuit boards by modified supercritical carbon dioxide combined with supercritical water pre-treatment. J CO_2 Util 41: 101265. https://doi.org/10.1016/j.jcou.2020.101265

Hao J, Wang Y, Wu Y, Guo F (2020) Metal recovery from waste printed circuit boards: A review for current status and perspective. Resour Conserv Recycl 157: 104787. https://doi.org/10.1016/j.proenv.2012.10.077

Mdlovu NV, Chiang CL, Lin KS, Jeng RC (2018) Recycling copper nanoparticles from printed circuit board waste etchants via a microemulsion process. J Clean Prod 185: 781-796. https://doi.org/10.1016/j.jclepro.2018.03.087

Kakria K, Thirumalini S, Secco M, Priya TS (2020) A novel approach for the development of sustainable hybridized geopolymer mortar from waste printed circuit boards. Resour Conserv Recycl 163: 105066. https://doi.org/10.1016/j.resconrec.2020.105066

Kang SH, Lee J, Chang JH (2010) Highly ordered ferromagnetic mesoporous materials: thermal phase transformation pathway and quantitative determination. J Phys Chem. C 114: 12440-12445. https://doi.org/10.1021/jp1028307

Kim YM, Han TU, Watanabe C, Teramae N, Park YK, Kim S, Wang BH (2015) Analytical pyrolysis of waste paper laminated phenolic-printed circuit board (PLP-PCB). J Anal Appl Pyrol 115: 87-95. https://doi.org/10.1016/j.jaap.2015.06.013

Kim JW, Lee AS, Yu S, Han JW (2018) En masse pyrolysis of flexible printed circuit board wastes quantitatively yielding environmental resources. J Hazard Mater 342:

438 51-57. https://doi.org/10.1016/j.jhazmat.2017.08.010
439 Liu JX, Jiang QH, Wang HL, Li JP, Zhang WJ (2021) Catalytic effect and mechanism
440 of in-situ metals on pyrolysis of FR4 printed circuit boards: Insights from kinetics
441 and products. Chemosphere 208: 130804.
442 https://doi.org/10.1016/j.chemosphere.2021.130804
443 Ma C, Yu J, Chen T, Yan Q, Song Z, Wang B, Sun L (2018) Influence of Fe based ZSM-
444 5 catalysts on the vapor intermediates from the pyrolysis of brominated acrylonitrile-
445 butadiene-styrene copolymer (Br-ABS). Fuel 230: 390-396.
446 https://doi.org/10.1016/j.fuel.2018.05.077
447 Masset P, Poinso JY, Poignet JC (2006) TG/DTA/MS study of the thermal
448 decomposition of $FeSO_4 \cdot 6H_2O$. J Therm Anal Calorim 83(2): 457-462.
449 https://doi.org/10.1007/s10973-005-7267-6
450 Nekouei R, Tudela I, Pahlevani F, Sahajwalla V (2020) Current trends in direct
451 transformation of waste printed circuit boards (WPCBs) into value-added materials
452 and products. Curr Opin Green Sustain Chem 24: 14-20.
453 https://doi.org/10.1016/j.cogsc.2020.01.003
454 Ning C, Hadi P, Aghdam E, Zhu S, Hui DCW, Lin CSK, G McKay (2017)
455 Environmental emission analysis of a waste printed circuit board-derived adsorbent
456 production process. Chem Eng J 326: 594-602.
457 https://doi.org/10.1016/j.cej.2017.05.181
458 Ng EP, Delmotte L, Mintova S (2009) Selective capture of water using microporous
459 adsorbents to increase the lifetime of lubricants. Chem Sus Chem 2: 255-260.

https://doi.org/10.1002/cssc.200800234

Qiu R, Lin M, Ruan J, Fu Y, Hu J, Deng M, Tang Y, Qiu R (2020) Recovering full metallic resources from waste printed circuit boards: A refined review. J Clean Prod 244: 118690. https://doi.org/10.1016/j.jclepro.2019.118690

Quan C, Li A, Gao N (2010) Synthesis of carbon nanotubes and porous carbons from printed circuit board waste pyrolysis oil. J Hazard Mater 179: 911-917. https://doi.org/10.1016/j.jhazmat.2010.03.092

Rajagopal RR, Aravinda LS, Rajarao R, Bhat BR, Sahajwalla V (2016) Activated carbon derived from non-metallic printed circuit board waste for supercapacitor application. Electrochim Acta, 211: 488-498. https://doi.org/10.1016/j.electacta.2016.06.077

Salbidegoitia JA, Fuentes-Ordóñez EG, González-Marcos MP, González-Velasco JR, Bhaskar T, Kamo T (2015) Steam gasification of printed circuit board from e-waste: Effect of coexisting nickel to hydrogen production. Fuel Processing Technol 133: 69-74. https://doi.org/10.1016/j.fuproc.2015.01.006

Siriwardane RV, Poston JA Jr., Fisher EP, Shen MS, Miltz AL (1999) Decomposition of the sulfates of copper, iron (II), iron (III), nickel, and zinc: XPS, SEM, DRIFTS, XRD, and TGA study. Appl Surf Sci 152(3-4): 219-236. https://doi.org/10.1016/S0169-4332(99)00319-0

Shen Y, Chen X, Ge X, Chen M (2018) Chemical pyrolysis of E-waste plastics: Char characterization. J Environ Manage 214: 94-103. https://doi.org/10.1016/j.jenvman.2018.02.096

482 Shen Y, Chen X, Ge X, Chen M (2018) Thermochemical treatment of non-metallic
483 residues from waste printed circuit board: Pyrolysis vs. combustion. J Clean Prod 176:
484 1045-1053. https://doi.org/10.1016/j.jclepro.2017.11.232
485 Shen YF (2020) A review on hydrothermal carbonization of biomass and plastic wastes
486 to energy products. Biomass Bioenergy 134: 105479.
487 https://doi.org/10.1016/j.biombioe.2020.105479
488 Terakado O, Ohhashi R, Hirasawa M (2011) Thermal degradation study of
489 tetrabromobisphenol A under the presence metal oxide: Comparison of bromine
490 fixation ability. J Anal Appl Pyrol 91: 303-309.
491 https://doi.org/10.1016/j.jaap.2011.03.006
492 Wu X, Zhu Y, Pei B, Cai P, Huang Z (2018) Effects of $FeCl_2$ on the pore structure of
493 porous carbon obtained from phenol formaldehyde resin and ethylene glycol. Mater
494 Lett 215: 50-52. https://doi.org/10.1016/j.matlet.2017.12.049
495 Xu Z, Tian D, Sun Z, Zhang D, Zhou Y, Chen W, Deng H (2019) Highly porous
496 activated carbon synthesized by pyrolysis of polyester fabric wastes with different
497 iron salts: Pore development and adsorption behavior. Colloids Surf A 565: 180-187.
498 https://doi.org/10.1016/j.colsurfa.2019.01.007
499 Yin J, Li GM, He WZ, Huang JW, Xu M (2011) Hydrothermal decomposition of
500 brominated epoxy resin in waste printed circuit board. J Anal Appl Pyrol 92: 131-136.
501 https://doi.org/10.1016/j.jaap.2011.05.005
502 Yousef S, Tatariants M, Tichonovas M, Bendikiene R, Denafas G (2018) Recycling of
503 bare waste printed circuit boards as received using an organic solvent technique at a

low temperature. J Clean Prod 187: 780-788.
https://doi.org/10.1016/j.jclepro.2018.03.227
Zhou YH, Wu WB, Qiu KQ (2011) Recycling of organic materials and solder from waste printed circuit boards by vacuum pyrolysis-centrifugation coupling technology. Waste Manage 31(12): 2569-2576. https://doi.org/10.1016/j.wasman.2011.07.002
Zhu X, Nie C, Wang S, Xie Y, Zhang H, Lyu X, Qiu J, Li L (2020) Cleaner approach to the recycling of metals in waste printed circuit boards by magnetic and gravity separation. J Clean Prod 248:119235. https://doi.org/10.1016/j.jclepro.2019.119235
Zhang YJ, Ou JL, Duan ZK, Xing ZJ, Wang Y (2015) Adsorption of Cr (VI) on bamboo bark-based activated carbon in the absence and presence of humic acid, Colloids Surf A 481:108-116. https://doi.org/10.1016/j.colsurfa.2015.04.050

Figures

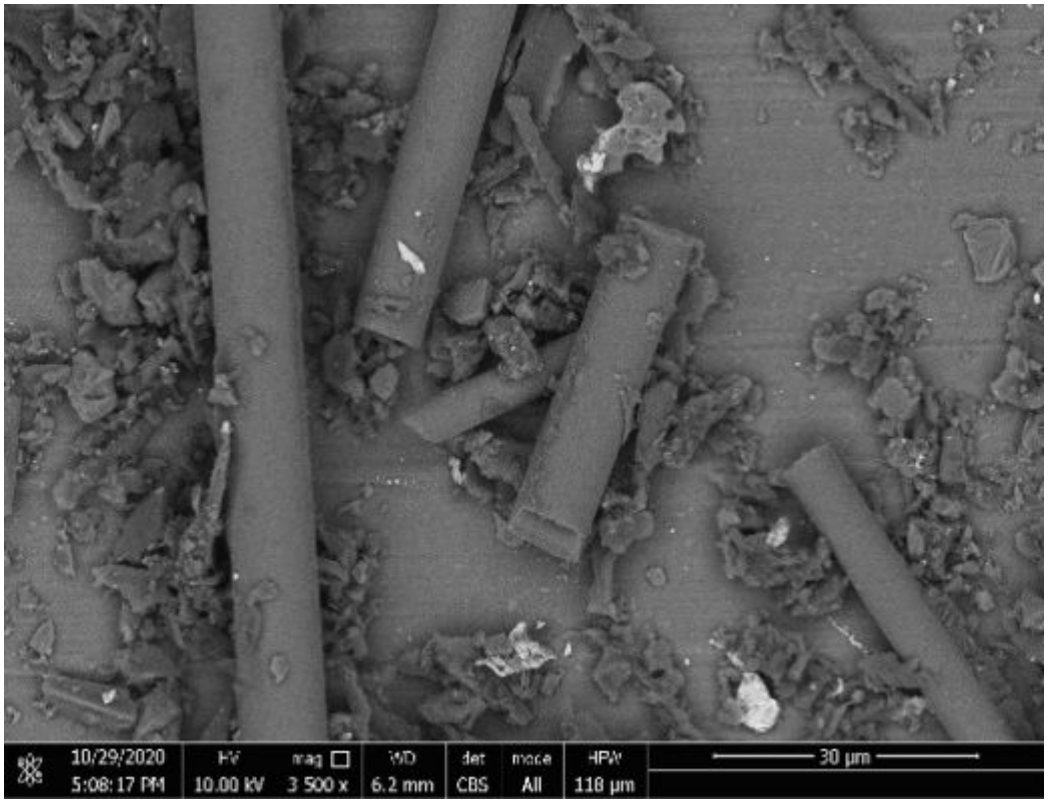

Figure 1

SEM image of the original WPCB

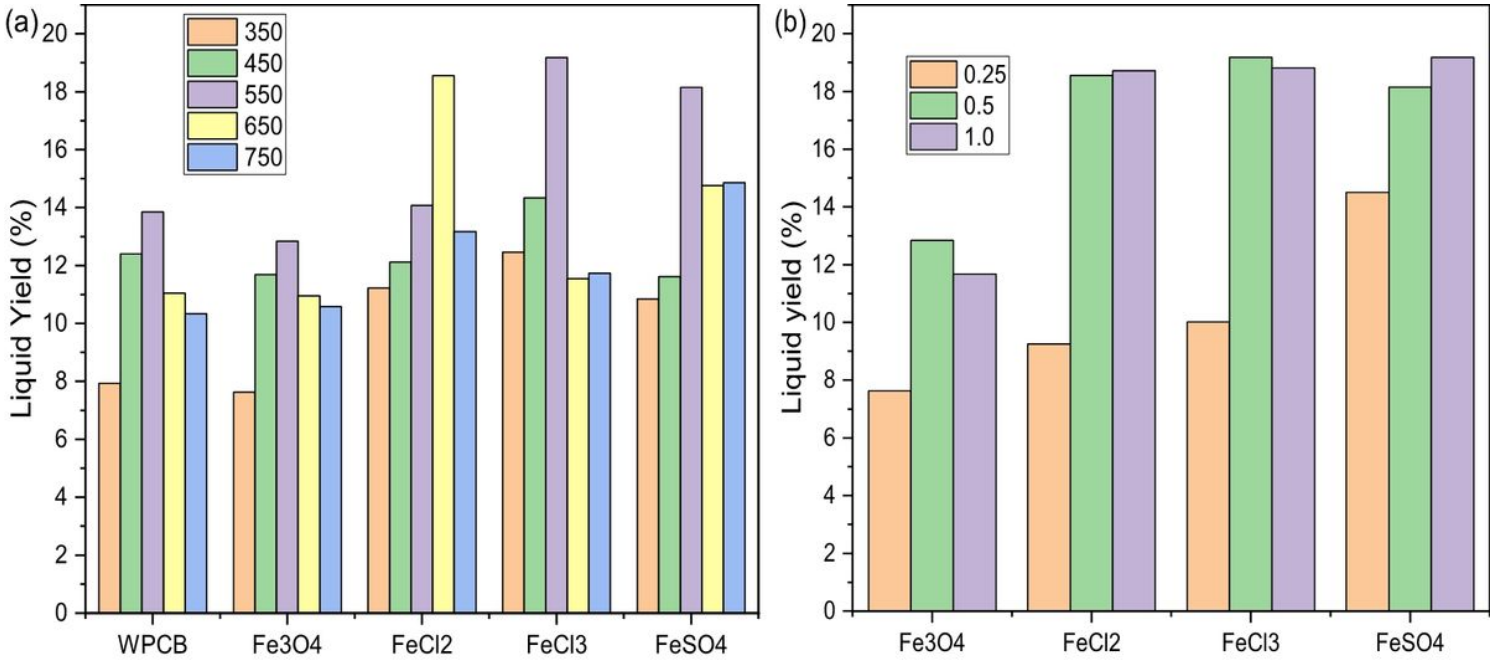

Figure 2

Liquid yield of WPCB with different iron compounds with the change of (a) temperature and (b) mass ratio

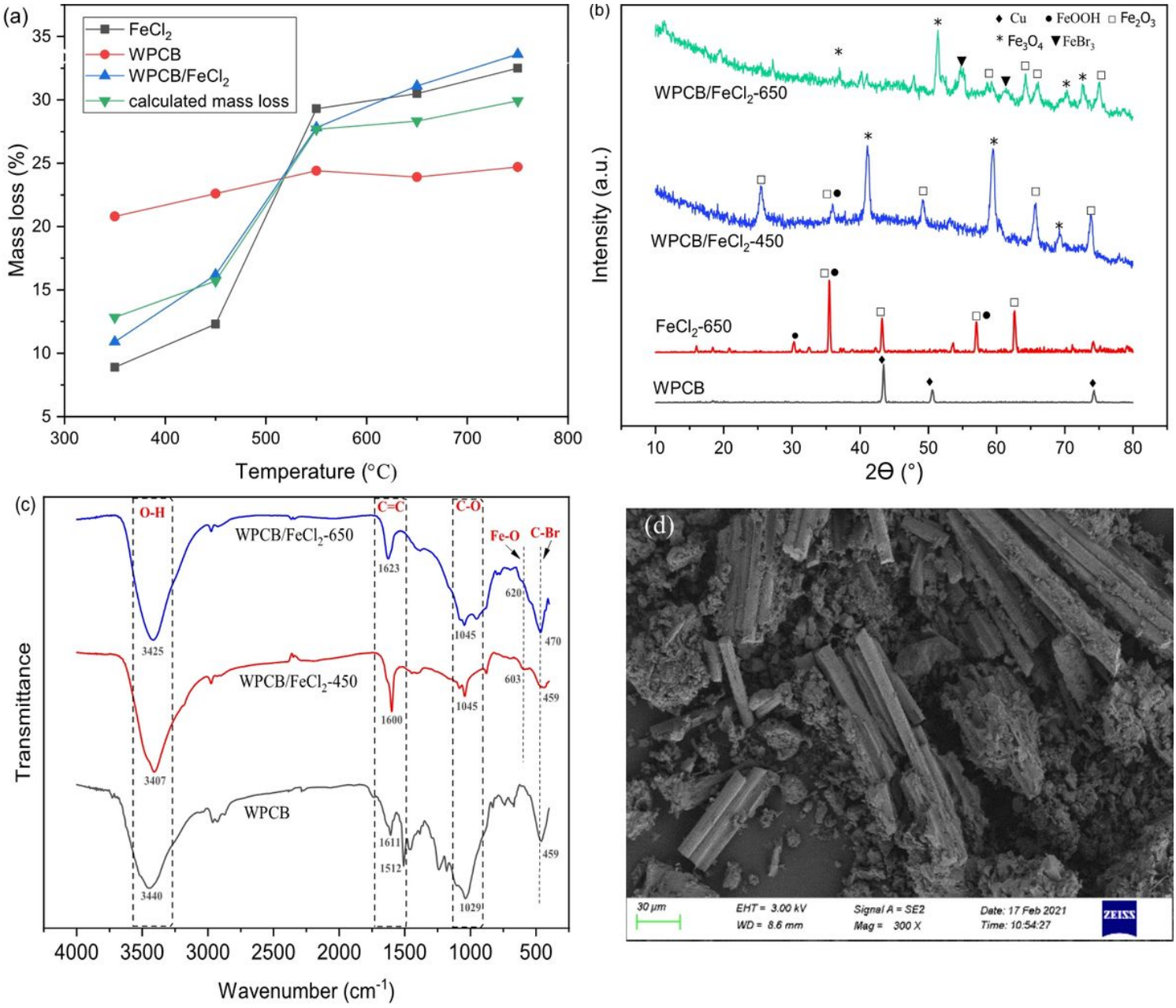

Figure 3

Characterization of WPCB, FeCl2 and WPCB/FeCl2: (a) mass loss; (b) XRD; (c) FTIR; (d) SEM image of WPCB/FeCl2-650

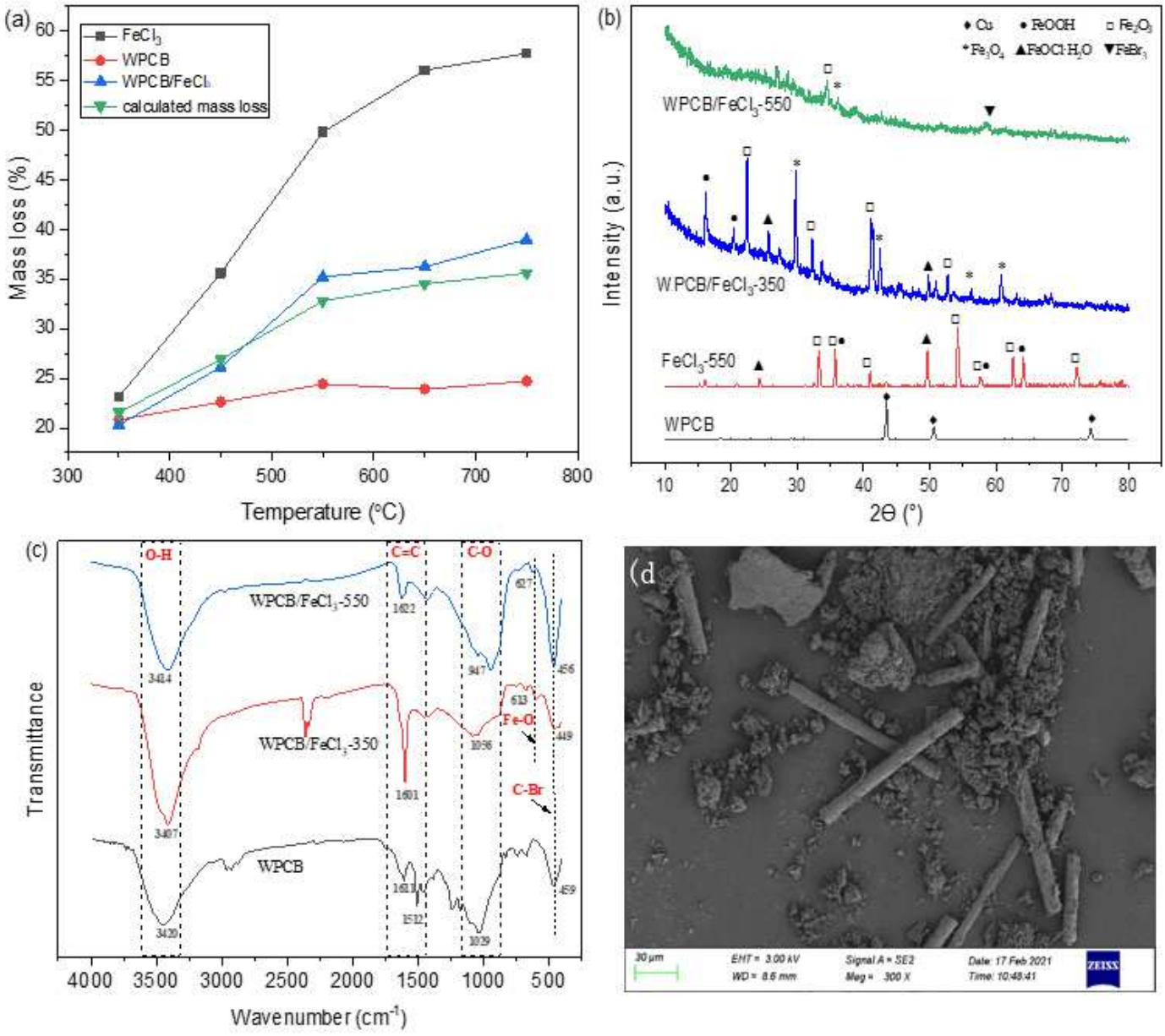

Figure 4

Characterization of WPCB, FeCl3 and WPCB/FeCl3: (a) mass loss; (b) XRD; (c) FTIR; (d) SEM image of WPCB/FeCl3-550

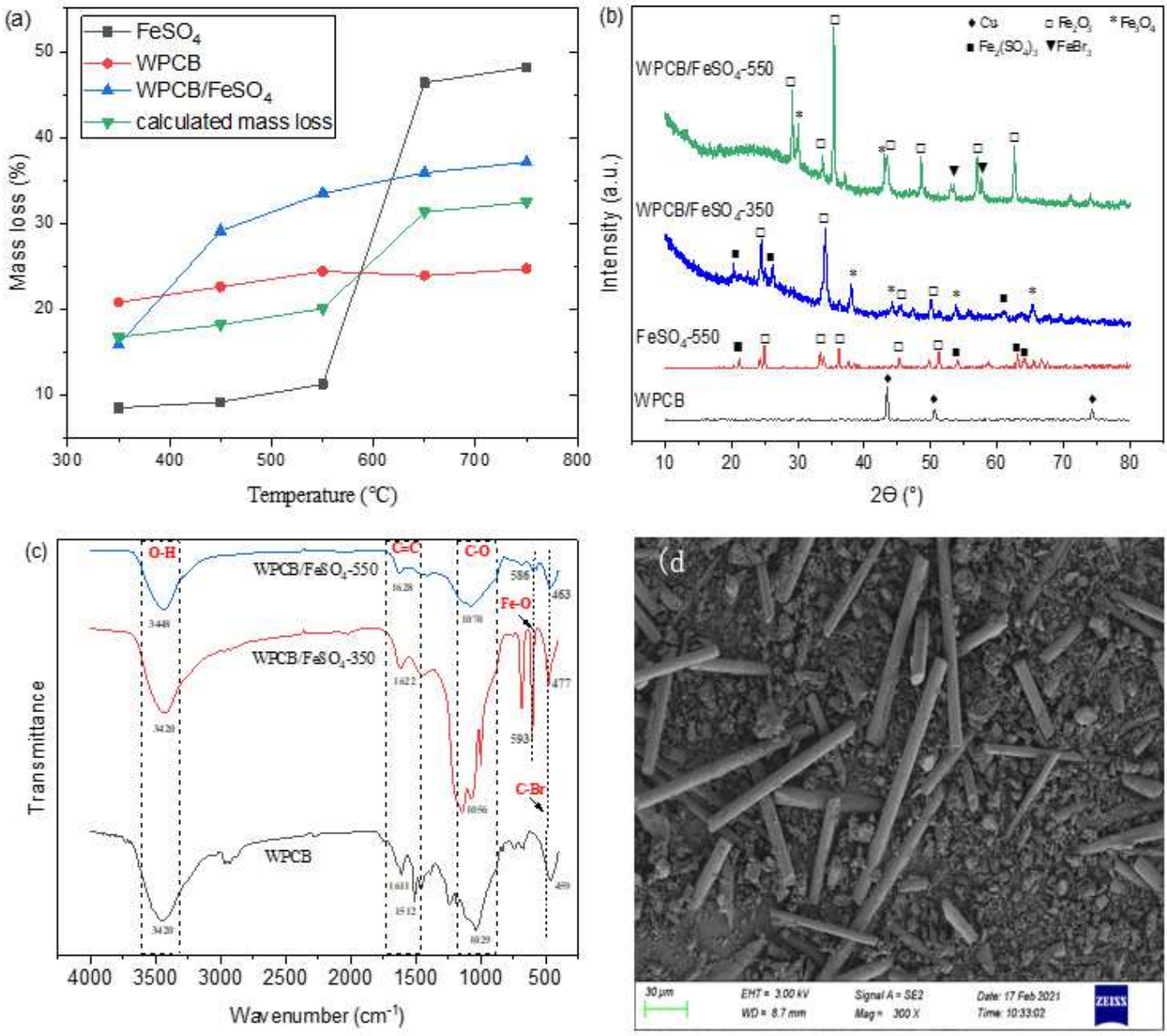

Figure 5

Characterization of WPCB, FeSO4 and WPCB/FeSO4: (a) mass loss; (b) XRD; (c) FTIR; (d) SEM image of WPCB/FeSO4-550

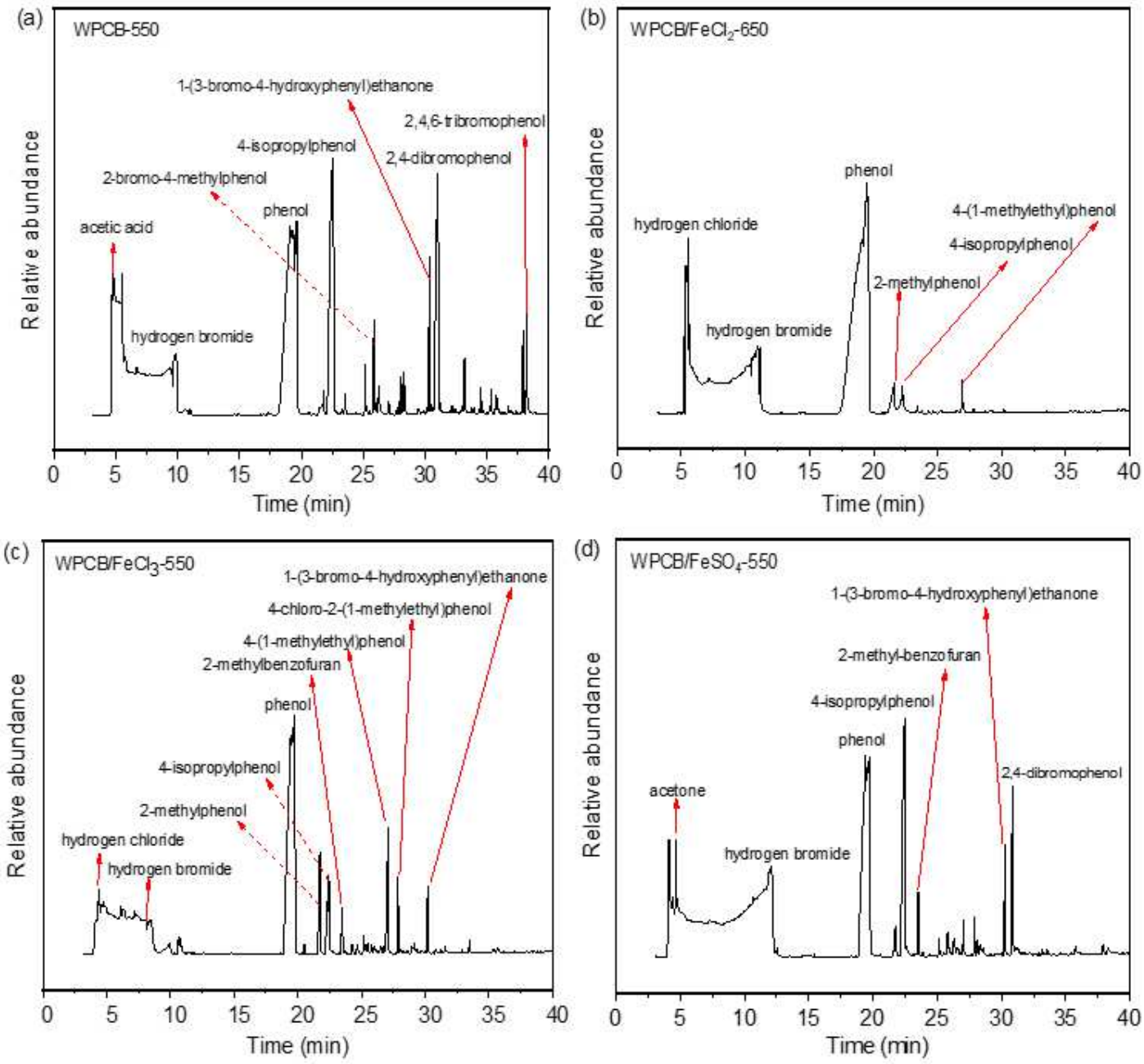

Figure 6

GC-MS results for pyrolysis liquid from (a) WPCB-550; (b) WPCB/FeCl2-650; (c) WPCB/FeCl3-550; (d) WPCB/FeSO4-550